Substantial brown carbon emissions from wintertime residential wood burning over France

Yunjiang Zhang, Alexandre Albinet, Jean-Eudes Petit, Véronique Jacob, Florie Chevrier, Gregory Gille, Sabrina Pontet, Eve Chretien, Marta Dominik-Sègue, Gilles Levigoureux, et al.

Science of the Total Environment 743 (2020) 140752

Contents lists available at ScienceDirect

Science of the Total Environment

journal homepage: www.elsevier.com/locate/scitotenv

Substantial brown carbon emissions from wintertime residential wood burning over France

Yunjiang Zhang [a,b,*], Alexandre Albinet [a,c], Jean-Eudes Petit [b], Véronique Jacob [d], Florie Chevrier [e], Gregory Gille [f], Sabrina Pontet [g], Eve Chrétien [h], Marta Dominik-Sègue [i], Gilles Levigoureux [j], Griša Močnik [k,l], Valérie Gros [b], Jean-Luc Jaffrezo [d], Olivier Favez [a,c,**]

[a] Institut National de l'Environnement Industriel et des Risques, 60550 Verneuil-en-Halatte, France
[b] Laboratoire des Sciences du Climat et de l'Environnement, CNRS-CEA-UVSQ, Université Paris-Saclay, 91191 Gif-sur-Yvette, France
[c] Laboratoire Central de Surveillance de la Qualité de l'Air (LCSQA), F-60550 Verneuil-en-Halatte, France
[d] Univ. Grenoble Alpes, CNRS, IRD, INP-G, IGE (UMR 5001), 38000 Grenoble, France
[e] Atmo Nouvelle Aquitaine, 17180 Perigny, France
[f] Atmo Sud, 13294 Marseille, France
[g] Atmo Auvergne Rhône-Alpes, 69500 Bron, France
[h] Atmo Grand Est, 67300 Schiltigheim, France
[i] Atmo Normandie, 76000 Rouen, France
[j] Air Pays de la Loire, 44300 Nantes, France
[k] Univ. of Nova Gorica, Center for Atmos. Research, Ajdovščina, Slovenia
[l] J. Stefan Institute, Condensed Matter Physics Dpt., Ljubljana, Slovenia

HIGHLIGHTS

- High contribution of brown carbon to aerosol absorption was observed at nine locations in France during winter.
- Major sources of brown carbon were attributed to wood burning emissions from residential heating.
- Mass absorption cross section of less oxidized BBOA was higher than that of the more oxidized.

GRAPHICAL ABSTRACT

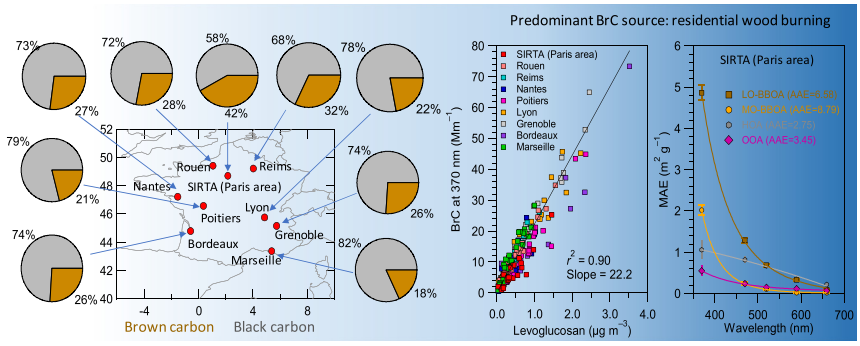

ARTICLE INFO

Article history:
Received 11 May 2020
Received in revised form 29 June 2020
Accepted 3 July 2020
Available online 6 July 2020

Editor: Jianmin Chen

Keywords:
Brown carbon
Multi sites

ABSTRACT

Brown carbon (BrC) is known to absorb light at subvisible wavelengths but its optical properties and sources are still poorly documented, leading to large uncertainties in climate studies. Here, we show its major wintertime contribution to total aerosol absorption at 370 nm (18–42%) at 9 different French sites. Moreover, an excellent correlation with levoglucosan ($r^2 = 0.9$ and slope = 22.2 at 370 nm), suggesting important contribution of wood burning emissions to ambient BrC aerosols in France. At all sites, BrC peaks were mainly observed during late evening, linking to local intense residential wood burning during this time period. Furthermore, the geographic origin analysis also highlighted the high potential contribution of local and/or small-regional emissions to BrC. Focusing on the Paris region, twice higher BrC mass absorption efficiency value was obtained for less oxidized biomass burning organic aerosols (BBOA) compared to more oxidized BBOA (e.g., about 4.9 ± 0.2 vs. 2.0 ± 0.1 $m^2\ g^{-1}$, respectively, at 370 nm). Finally, the BBOA direct radiative effect was found to be 40% higher

* Correspondence to: Yunjiang Zhang, Institut National de l'Environnement Industriel et des Risques, 60550 Verneuil-en-Halatte, France.
** Corresponding author.
E-mail addresses: yjanzhang@gmail.com (Y. Zhang), olivier.favez@ineris.fr (O. Favez).

https://doi.org/10.1016/j.scitotenv.2020.140752
0048-9697/

Residential wood burning
Mass absorption efficiency
France

when these two BBOA fractions are treated as light-absorbing species, compared to the non-absorbing BBOA scenario.

1. Introduction

Carbonaceous aerosols, consisting of black carbon (BC) and organic matter (OM), account for a substantial fraction of atmospheric fine aerosols (Zhang et al., 2007). They have both direct and indirect effects on the Earth's energy budget and thus on climate change (Bond et al., 2013; IPCC, 2013). BC is known as a major absorber of solar radiation from the ultraviolet to the infrared part of the spectrum. Part of organic aerosols (OA), so-called brown carbon (BrC) (Andreae and Gelencsér, 2006), can also absorbs solar radiation, mainly in the ultraviolet region (Laskin et al., 2015; Moise et al., 2015). While BC absorption is relatively well characterized, the knowledge on sources and optical properties of BrC remains limited, inducing large uncertainties in the radiative forcing assessment at the global scale (Saleh, 2020; Saleh et al., 2015).

Atmospheric BrC can be emitted by primary sources or formed by secondary processes, involving anthropogenic and biogenic origins (Laskin et al., 2015; Moise et al., 2015). Regarding primary emissions, combustion sources have been widely demonstrated as substantial BrC contributors at various types of locations (Chen et al., 2020; de Sá et al., 2019; Moschos et al., 2018; Qin et al., 2018; Washenfelder et al., 2015; Xie et al., 2019). Globally, open biomass burning (e.g., fire emissions) was reported as an important BrC source (Saleh et al., 2015). In particular, residential wood burning - which is now recognized as a predominant wintertime OA source in Western Europe within emission inventories (Denier van der Gon et al., 2015) - has been assessed as a major source of BrC at various urban (Favez et al., 2009; Moschos et al., 2018; Zhang et al., 2018) and rural (Golly et al., 2019) environments. Moreover, a growing number of studies are also indicating significant contributions of secondary organic aerosols (SOA) to BrC concentrations, while comprehensive source apportionment exercises of light absorbing OA are still needed (Chen et al., 2018; Gilardoni et al., 2016; Kumar et al., 2018; Lambe et al., 2013; Moise et al., 2015; Moschos et al., 2018; Xie et al., 2020).

The carbonaceous aerosols' contribution to radiative budget is not only determined by its total burden in the atmosphere, it is also largely affected by the specific optical properties of the different types of light absorbing compounds. These properties are commonly investigated via the aerosol absorptivity (Romonosky et al., 2019; Saleh et al., 2014) and absorption coefficients are usually normalized by the mass of absorbing particles to determine the wavelength-dependent mass absorption efficiency (MAE) (Bond et al., 2013). The MAE is further applied in climate models to explain the relationship between radiative impacts and concentrations of a given aerosol type (Bond et al., 2013). BrC MAE can span several orders of magnitude according to the different types of aerosols from various sources observed in different regions (Chen et al., 2020; de Sá et al., 2019; Kumar et al., 2018; Laskin et al., 2015; Moschos et al., 2018; Qin et al., 2018; Washenfelder et al., 2015). However, most climate models still roughly treat OA as non-absorbing aerosols (Li et al., 2016; Saleh, 2020), since the main sources and light-absorption properties (e.g., MAE) of brown carbon in the ambient air remain poorly understood.

In this context, we investigated the relationship between BrC light absorption (measured using multi-wavelength aethalometer) and biomass burning aerosols in winter at nine (peri-)urban sites distributed over France and so, under various climatic conditions. We also benefited of high-time resolution OA source apportionment (based on quadrupole aerosol chemical speciation monitor (ACSM) measurements) at one of these sites (located in the Paris region) to estimate component-specific BrC MAE using multiple linear regression (MLR) analysis. Finally, we evaluated the potential radiative forcing effect of two types of biomass burning-related OA.

2. Materials and methods

2.1. Sampling site and measurements

Online measurements and filter samplings were performed during the 2014–2015 winter season at different urban areas over France, including Rouen, Reims, greater Paris (SIRTA), Nantes, Poitiers, Lyon, Grenoble, Bordeaux, and Marseille (see Fig. 1 and Table S1). All these sites correspond to urban background stations operated by regional air quality monitoring networks, except for the SIRTA facility, which is part of the European Research Infrastructure for the observation of Aerosol, Clouds and Trace gases (ACTRIS). This research platform is located 25 km southwest from the Paris city center and is representative of the background for the determination of air quality within the Paris region.

Spectral dependence of aerosol light absorption coefficients was measured at all sites using a seven-wavelength (370, 470, 520, 590, 660, 880, and 950 nm) Aethalometer (Magee scientific, AE33, $PM_{2.5}$ size cut-off, 5 L min^{-1} and 1 min time resolution). This instrument notably allows for the automatic correction of the so-called filter loading effect, as detailed in (Drinovec et al., 2017; Drinovec et al., 2015). Briefly, the sampled ambient air is divided and the sample is deposited onto two filter spots at different flowrates, leading to uneven loadings on the respective filter spots. A compensation parameter k is retrieved from the different loading effect magnitudes influencing these two spots, and k is further used to determine the light attenuation (b_{ATN}) due to carbonaceous aerosols. Absorption coefficients (b_{abs}) are eventually obtained at each wavelength following Eq. (1):

$$b_{abs} = \frac{b_{ATN}}{C} \quad (1)$$

where C represents the overall filter multiple-scattering enhancement parameter (Drinovec et al., 2015). In accordance with previous studies at SIRTA (Zhang et al., 2018; Zhang et al., 2019) and other ACTRIS sites (Zanatta et al., 2016), a wavelength independent C value of 2.57 was applied to AE33 data measured at each site of the present study. At SIRTA, the data of equivalent mass concentration of wood burning BC (eBC_{wb}) used in the present study was obtained from our previous study (Zhang et al., 2019).

Meanwhile, concentrations of levoglucosan - commonly used as a marker for biomass burning aerosols (Simoneit, 2002) - was obtained from off-line analysis of PM_{10} filter samples collected using DAH-80 high volume samplers at a flow rate of 30 m^3 h^{-1} (Digitel) at all sites. Filters were collected on a daily time-base, near-continuously from mid-November 2014 to mid-April 2015, and a part of them was analyzed. The selection of filters to be analyzed (with a total number ranging from 24 to 50 filters, depending on the site) was achieved to obtain a good temporal representativity of the investigated period (typically every third day) but also according to the actual filter availability as well as the availability of co-located AE33 data. Levoglucosan quantification was performed using high-performance liquid chromatography followed by amperometric detection (HPLC-PAD) (Waked et al., 2014).

Finally, concentrations of non-refractory major chemical species within submicron aerosol ($NR\text{-}PM_1$) have been continuously measured at SIRTA using the ACSM (Aerodyne Res. Inc.) at a time resolution of

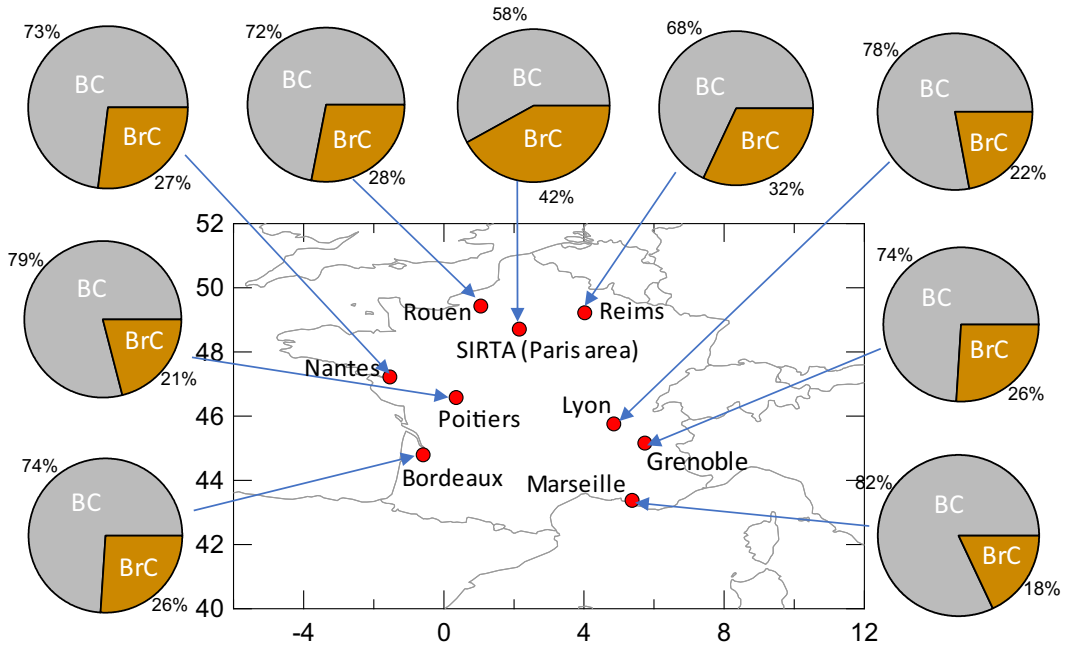

Fig. 1. Contributions of black carbon (BC) and brown carbon (BrC) to total aerosol absorption at 370 nm observed across France during the 2014–2015 winter season.

approximately 30 min. These measurements notably include the OA fraction and its mass spectra. Detailed descriptions of the ACSM and its set-up at SIRTA can be found elsewhere (Ng et al., 2011; Zhang et al., 2019).

2.2. Determination of BrC absorption coefficients

The wavelength dependence of BrC absorption coefficients ($b_{BrC,\lambda}$) was calculated assuming that BC is the only absorber at 880 nm. The absorption Ångström exponent (AAE) is a widely used parameter that describes the wavelength (λ) dependence of aerosol light absorption (Eq. (2)). The spectral dependence of BC absorption ($b_{BC,\lambda}$) can be derived based on the measured total aerosol absorption coefficients ($b_{total,\lambda}$) using Eq. (3) (Kumar et al., 2018). BC AAE values usually range between 0.9 and 1.1 (Bond et al., 2013; Lu et al., 2015). In this study, an AAE of 1 was applied for the estimation of $b_{BC,\lambda}$, which is notably consistent with previous studies at SIRTA (Zhang et al., 2018). To evaluate impact of this BC AAE value range on quantification of BrC, we performed a sensitivity test using the BC AAE values at 0.9, 1, and 1.1, respectively (see Fig. S1). As indicated by the result of this sensitivity test, an uncertainty (ratio of standard deviation to mean) of approximately 11% at 370 nm was observed when using these different AAE values to calculate BrC. Finally, the $b_{BrC,\lambda}$ at 370, 470, 520, 590, and 660 nm could be calculated following Eq. (4):

$$AE(\lambda_1,\lambda_2) = \frac{In(b_{abs,\lambda_1}) - In(b_{abs,\lambda_2})}{In(\lambda_1) - In(\lambda_2)} \quad (2)$$

$$b_{BC,\lambda} = b_{tot,880nm} \times \left(\frac{880\ nm}{\lambda}\right)^{AAE} \quad (3)$$

$$b_{BrC,\lambda} = b_{tot,\lambda} - b_{BC,\lambda} \quad (4)$$

2.3. Source apportionment of OA

Prevalent OA sources at SIRTA were resolved by positive matrix factorization (PMF) (Paatero and Tapper, 1994) applied to ACSM organic mass spectra, using the source finder (SoFi) toolkit (Canonaco et al., 2013) equipped with a multilinear engine (ME-2) (Paatero, 1999). More description about PMF can be found in Text S1. Considering to large interferences of internal standard of naphthalene at m/z's 127–129 – which may provide some uncertainties for the PMF analysis – only $m/z < 100$ was used here for the ME-2 analysis (Zhang et al., 2019). As reported by our previous study (Zhang et al., 2019), two major POA sources, i.e., traffic (HOA) and biomass burning (BBOA) emissions, were identified at SIRTA across a long-term period (six years). Although a single BBOA factor was chosen as the "best estimate" for the PMF runs in the context of such a multi-year investigation (Zhang et al., 2019), two types of wood burning organic aerosols (i.e., less and oxidized BBOA) – which have been identified using high resolution aerosol mass spectrometer PMF method during cold seasons at SIRTA (Crippa et al., 2013; Fröhlich et al., 2015) – could be expected when, focusing only on the winter period. To further explain the different types of BBOA factors, the reference mass spectral profiles of the two BBOA (Crippa et al., 2013; Fröhlich et al., 2015) has been applied in the present ME-2 analysis to constrain these factors. The mass spectrum of HOA was also constrained using the one mainly related traffic source from (Crippa et al., 2013), while an oxygenated OA (OOA) factor was unconstrued. Overall, the four-factor solution was resolved in the present study to account for the OA components in winter, including HOA, less (LO-BBOA) or more (MO-BBOA) oxidized biomass burning OA, and OOA. More discussion on these OA factors has been given in Section 3.3.

2.4. Air mass back trajectory analysis

The 72-h back trajectories of air masses arriving at each sampling site at a height of 100 m above ground level were calculated every 1 h by using the HYbrid Single-Particle Lagrangian Integrated Trajectory model (Draxler and Rolph, 2003). The Global Data Assimilation System (GDAS) meteorological data was used for these calculations. The potential source contribution function (PSCF) (Polissar et al., 1999) was applied here to evaluate possible geographic origins of high absorption coefficients of brown carbon. As the PMF OA factors were available at SIRTA (Paris area), the PSCF analysis has been also applied to further understand the geographic sources of these OA factors. Briefly, to

determine the possibility of the geographic origin area, the probability function (i.e., PSCF) was calculated using Eq. (5). In this equation, i and j indicate latitude and longitude for a two-dimension grid cell (i, j), respectively. m_{ij} refers to the total number of selected trajectory endpoints (i, j) linked to the given observed absorption coefficients of brown carbon or mass concentrations of OA factors, which are higher than the threshold value (i.e., 75th percentile of each variable during the entire observation period). n_{ij} is the total number of trajectory endpoints at each grid cell (i, j). w_{ij} is an arbitrary weighting function (Waked et al., 2014), which is applied here to reduce uncertainty of PSCF modeling due to small n_{ij} values. The detailed description of this weighting function can be found in Waked et al. (2014). The grid resolution was set by 0.25° × 0.25°. The trajectory data was filtered by rainfall (higher than 1 mm h^{-1}) to reduce wet deposition impact, and was limited by the air mass altitude threshold up to 2000 m. The PSCF analysis was performed using an IGOR-based toolkit (ZeFir) (Petit et al., 2017).

$$PSCF_{(i,j)} = \left(\frac{m_{ij}}{n_{ij}}\right) \cdot w_{ij} \quad (5)$$

2.5. Determination of source-specific MAE

The MLR analysis was applied to determine MAE of the OA factors discussed hereabove, following:

$$b_{abs-BrC} = m_1 * [HOA] + m_2 * [LO-BBOA] + m_3 * [MO-BBOA] + m_4 * [OOA] + intercept \quad (6)$$

In Eq. (6), $b_{abs-BrC}$ indicates brown carbon absorption coefficient (Mm^{-1}) and the unit of these four OA factors is mass concentration (μg m^{-3}). All of these data are 1-h time resolution. The coefficients, intercepts, and standard deviation from the MLR analysis have been given in Table S2. Fig. S2 presents the correlations of brown carbon absorption coefficients ($b_{abs\text{-}BrC}$) between observed and calculated from the MLR method. Overall, excellent agreements (r^2 = 0.78–0.87, slope = 0.93–0.99) between the observation and the calculation at different wavelengths (including 370, 470, 520, 590, and 660 nm) are observed, highlighting negligible residual of the MLR analysis. More detailed discussion about the OA-factor-specific MAE values are given in Section 3.4.

3. Results and discussion

3.1. Multi-site measurements of BrC

The averaged total absorption coeffients at 370 nm ($b_{abs,370}$) ranged from approximately 13 to 53 Mm^{-1} for the different sites of the study (Table S1). As shown in Fig. 1, BrC contributed up to more than 40% to aerosol absorption at this wavelength. Highest mean contributions (32–42%) were mainly observed in Northeastern regions while the lowest one (18%) was obtained for the Southeastern site (Marseille). This spatial distribution is reflecting variations in the Angström Absorption Exponent (AAE, in the range 370–950 nm) values among those sampling sites (Table S3). Furthermore, as presented by Fig. 2, a very good correlation (r^2 = 0.90) has been observed between daily-averaged BrC absorption coeffients ($b_{BrC,370}$) and levoglucosan concentrations across all the sites. This latter result suggests the predominance of biomass-combustion source for ambient brown carbon during wintertime in France. As a matter of fact, the displayed $b_{BrC,370}$ diel profiles were consistent with those generally observed for residential wood burning aerosols (Favez et al., 2010; Sciare et al., 2011; Zhang et al., 2019), with late evening maxima (see Fig. 3) at all sampling sites.

All these observations are confirming the overwhelming influence of residential wood burning emissions on BrC loadings in France during wintertime. Accordingly, BrC absorption coefficients might then be considered as an accurate proxy for biomass burning aerosols during this period of the year. As shown in Table S3 and Fig. 4, AAE values of BrC in the lower wavelength range region (370–520 nm) are comparable from one investigated site to another, with a small standard deviation (4.80 ± 0.28, mean ± 1σ), suggesting that biomass burning organic aerosols have overall similar optical and/or chemical properties at those sites. Based on PM_{10} filter-based PMF analyses achieved for 15 different sites, Weber et al. (2019) found that levoglucosan accounts for 8 ± 2% of the total wood burning aerosol concentrations over France. Combining this number ($\frac{Levoglucosan}{PM_{10,wood\ burning}} = 8 \pm 2\%$) with the slope value obtained from Fig. 2 ($\frac{b_{BrC,370}}{Levoglucosan} = 22.2 \pm 0.4\ m^2\ g^{-1}$), we could propose a BrC-levoglucosan-tracer method to roughly estimate mass concentration of biomass burning aerosol concentrations ($PM_{10,wood\ burning}$), as illustrated by Fig. S3. To examine the validity of this method, we applied it to 2 independent datasets for which AE33 and levoglucosan data as well as PMF outputs were already available elsewhere. These datasets are corresponding to i) an intensive field campaign with 4 h-filter samplings during Spring 2015 at SIRTA (Srivastava et al., 2018) and ii) daily filter-based measurements in Metz (Petit et al., 2019). As shown in Fig. S3, a good correlation (r^2 = 0.83, slope = 1.11 ± 0.03, N = 227) was obtained between PMF wood burning factor and $PM_{10,wood\ burning}$, supporting the good performance of the BrC-levoglucosan-tracer method to quantify biomass burning source emissions. It should be noted that such a tracer method might be essentially applicable for conditions where biomass burning is the predominated source of ambient particulate brown carbon, for instance in France during cold seasons. Moreover, considering that the importance of biomass burning from residential wood burning sector has been widely recognized in western Europe (Crippa et al., 2014; Daellenbach et al., 2017; Denier van der Gon et al., 2015; Moschos et al., 2018), the performance and uncertainty of the BrC-levoglucosan-tracer method proposed here could be further evaluated at other locations in future studies.

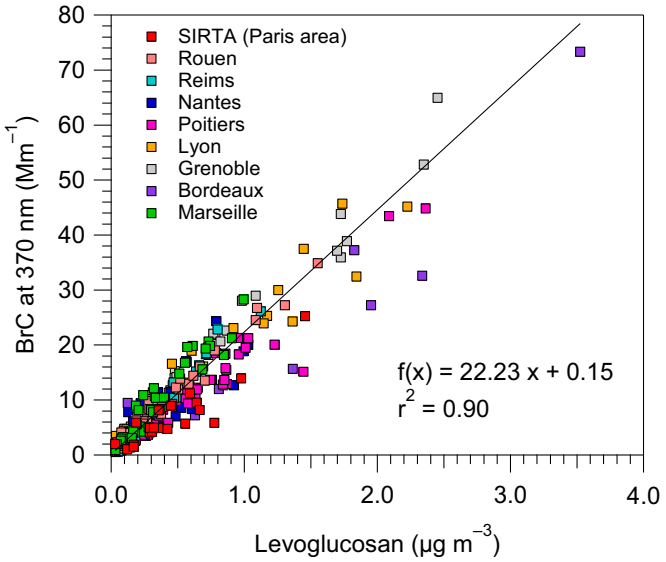

Fig. 2. Correlation between BrC absorption at 370 nm and levoglucosan concentrations measured at each site. The linear fit (orthogonal distance regression) has been obtained taken all data points into account.

3.2. Geographic origins of BrC

Fig. 5 shows maps for the PSCF analysis of brown carbon at different city sites. At SIRTA (Paris area), brown carbon presents high PSCF values

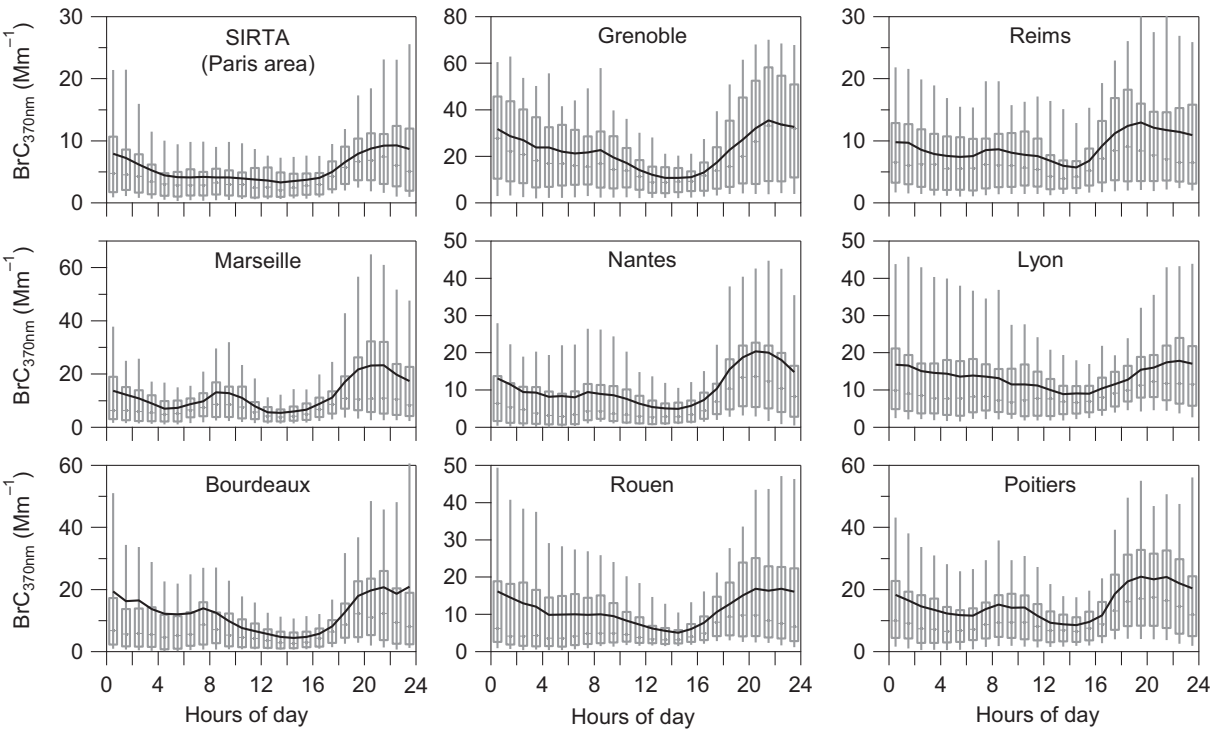

Fig. 3. Diurnal variations of BrC absorption coefficients at 370 nm observed at the 9 sampling sites. The upper and lower boundaries of boxes indicate the 75th and 25th percentiles, respectively; the lines within the box correspond to median values; the whiskers above and below boxes refer to 95th and 10th percentiles, respectively; and solid lines represent mean values.

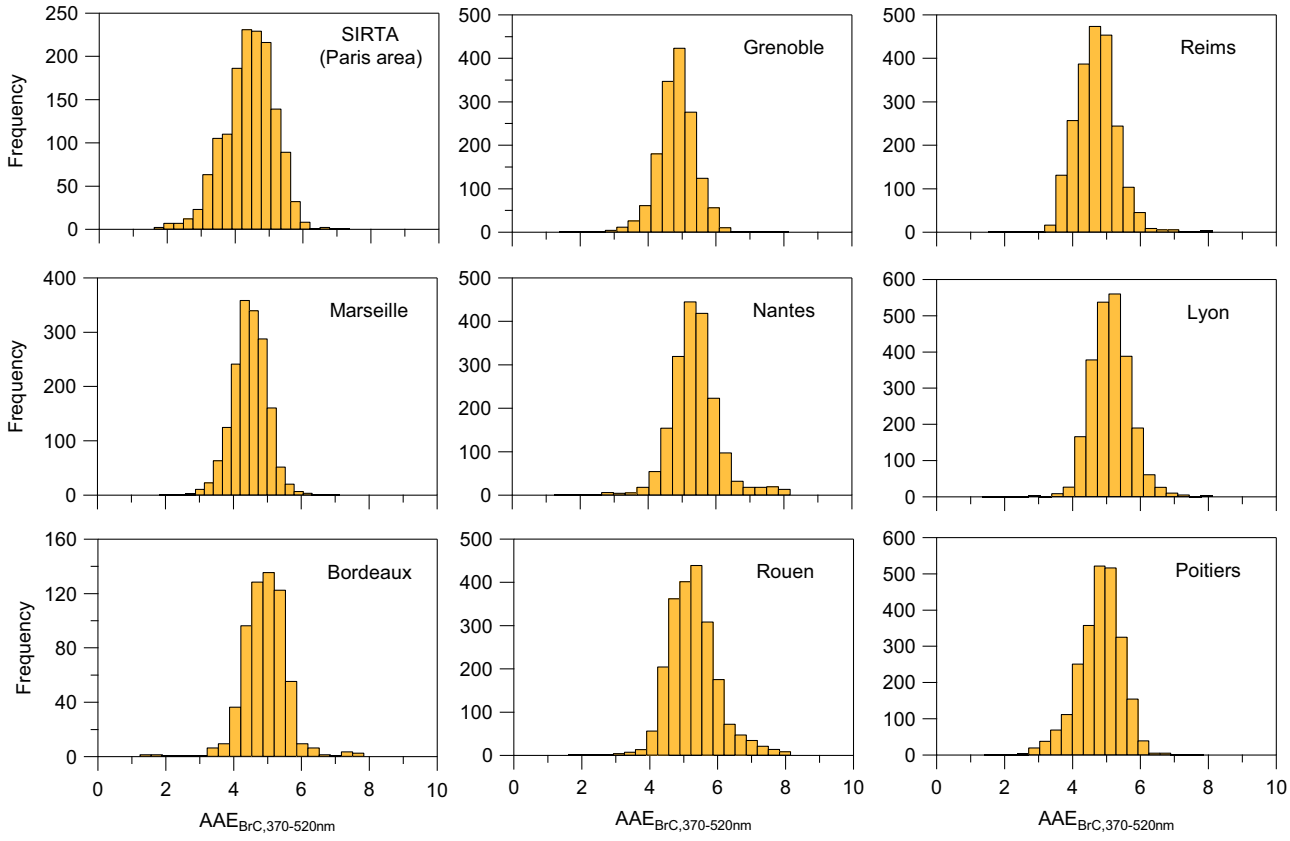

Fig. 4. Frequency distributions of brown carbon AAE values in the wavelength range 370–520 nm measured at different sites.

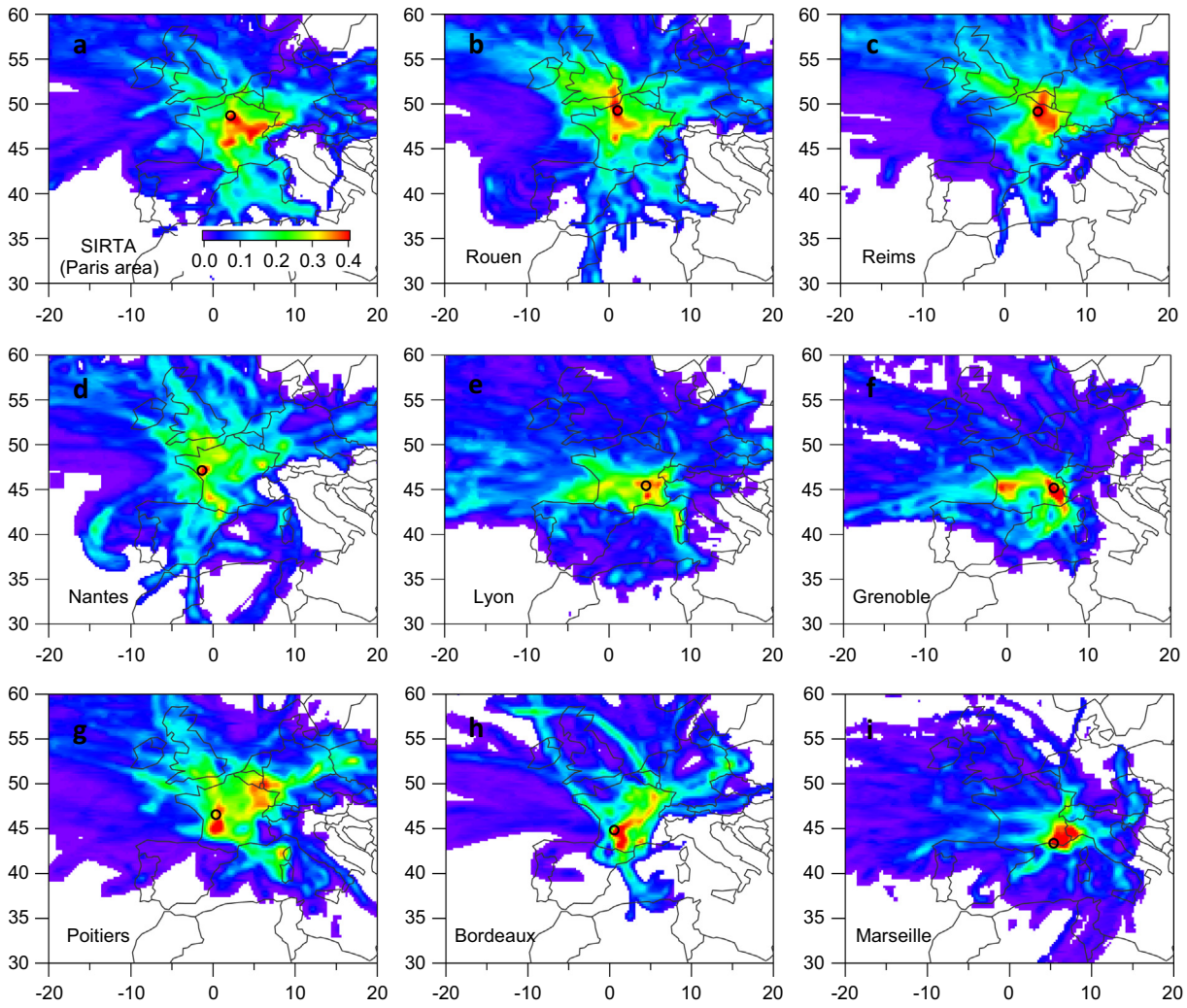

Fig. 5. Potential geographic sources of brown carbon at each site. The cities, i.e., (a) SIRTA (Paris area), (b) Rouen, (c) Reims, (d) Nantes, (e) Lyon, (f) Grenoble, (g) Poitiers, (h) Bordeaux, and (i) Marseille, are marked by hollow circles in each panel. The PSCF values are indicated by color scales, where a color scale bar is only shown in the top-left panel.

located to local scale and the southeast and south of the sampling site (Fig. 5a). This PSCF pattern is consistent with the high possible source region of BBOA factors observed in the present study (see further discussion in Section 3.3) and our previous study for multi-year winters (Zhang et al., 2019). These results suggest that both local emissions and regional transport could dominate the high loadings of brown carbon aerosols in the Paris region. As shown in Fig. 5b, the high-PSCF region of brown carbon is characterized with local scale and two distinct transport pathways, i.e., the southeast and northwest of Rouen, respectively. The former pathway is highly similar as the possible source region of brown carbon observed at SIRTA, indicating a similar geographic origin of high BrC loadings observed at the two city areas (i.e., Paris and Rouen). It should be noted that the latter pathway is originated from a region in the eastern UK, reflecting possible influence of biomass burning emissions and subsequent transport from the UK on ambient brown carbon aerosols observed in Rouen. As shown in Fig. 5c, the high potential origins of brown carbon are mainly located to local scale, the northern (e.g., originated from the northern region of Belgium) and the southeastern areas of Remis. These results highlight an important role of local emissions and regional transport in contributing to the high BrC loadings observed in Reims. As indicated by the PSCF analysis in these three city areas (i.e., Paris, Rouen, and Remis), the high potential geographic origins over the northeastern region in France could substantially contribute to atmospheric brown carbon during cold months.

At both Nantes and Lyon sites (Fig. 5d and e), the small region of high-PSCF values is observed predominantly from local scale. This suggests that local biomass burning emissions were an important source for the high loadings of brown carbon in these two city regions. As shown in Fig. 5f, there are two distinct hot spots of the high PSCF values observed in Grenoble. One is distributed at local scale, while another is related to regional transport originated from a region near Poitiers (see Fig. 5g). In Poitiers (Fig. 5g), an evident high-PSCF region of brown carbon is located to a small area from the south of the sampling site. Meanwhile, the relatively high PSCF values observed in Poitiers could be associated with the potential source origins of brown carbon observed in Reims (Fig. 5c). This might suggest a regional transport pathway of brown carbon aerosols from the northeast to the southwest of France. In addition to high potential source from a local scale, a narrow high-PSCF bond located to the northeast of the sampling site was observed in Bordeaux (Fig. 5h). This possible reginal transport is originated from the highly possible source region of brown carbon over the northeastern area of France (Figs. 5a–c). In Marseille (Fig. 5i), the high PSCF values are located to the local area and the region over Grenoble (Fig. 5f). This reflects that brown carbon observed in Marseille could be influenced by local emissions and regional transport originated from the Grenoble region.

Overall, these PSCF analysis highlighted that local emissions and regional transport could be a high potential source for high levels of brown carbon aerosols observed at these most receptor sites. Especially, wood burning emissions from local scale and/or short-distance transport may be a predominant geographic origin for brown carbon aerosols. Furthermore, the diel variations of brown carbon (see Fig. 3) – which are characterized by evident late evening peaks at all sampling sites – could further support important contribution of local emissions to brown carbon. These diel cycle patterns is also consistent with the variations of wood-burning aerosols (e.g., BBOA and eBC_{wb}) reported by some previous studies at various sites during cold months in France (Favez et al., 2009; Favez et al., 2010; Languille et al., 2020; Weber et al., 2019; Zhang et al., 2019), as well as the funding in this study (see Fig. 6). Interestingly, the BrC PSCF patterns described above seems coherent with the spatialized emission inventories available for residential wood burning in France (Denier van der Gon et al., 2015). All of these findings above could support that wood burning emissions from residential sector in France are a ubiquitous and important source for atmospheric brown carbon aerosols during wintertime.

3.3. Sources of organic aerosol at SIRTA

As shown in Fig. 6a, the mass spectrum of HOA is characterized by the dominating $C_xH^+_{2x+1}$ and $C_xH^+_{2x+1}$ ion family, which is generally associated with traffic-related POA in urban environment (Sun et al., 2011; Zhang et al., 2011). The diurnal cycle of the HOA factor presents two high peaks at morning and evening rush hours (Fig. 6b), mainly due to intense traffic emissions (Zhang et al., 2019). As shown in Fig. S4a, the mass concentration of HOA resolved in this study is excellently correlating ($r^2 = 0.99$) with the one from our previous study (Zhang et al., 2019). As shown in Fig. S4b, the difference of HOA between Zhang et al. (2019) and the present study is correlated well with wood burning black carbon aerosol (eBC_{wb}), demonstrating that the lower HOA in this study is mainly due to less biomass burning influence compared to Zhang et al. (2019). Hence, the new OA factor solution in this study could reduce influence, to some extent, of biomass burning emissions on such HOA factor (Zhang et al., 2019).

The mass spectrum of LO-BBOA presents strong signal fractions at *m/z* 29, 60 and 73, which is similar at the ones widely observed under ambient environments influenced by fresh biomass burning emissions (Cubison et al., 2011; de Sá et al., 2019; Lanz et al., 2010; Zhang et al., 2015). Compared to the LO-BBOA, MO-BBOA has lower *m/z* 60 and higher *m/z* 44 fractions in its mass spectrum (Fig. 6a), representing for a more oxidized or aged BBOA factor (Crippa et al., 2013; Cubison et al., 2011; de Sá et al., 2019; Zhang et al., 2015). As presented in Fig. 6b, both LO-BBOA and MO-BBOA show evidently high peaks during nighttime linking to enhanced residential wood burning emissions due to intense heating purpose. LO-BBOA and MO-BBOA have good correlations ($r^2 = 0.55$–0.69) with wood burning source tracer, i.e., eBC_{wb} (Figs. S4 c and d). Moreover, the sum of LO-BBOA and MO-BBOA

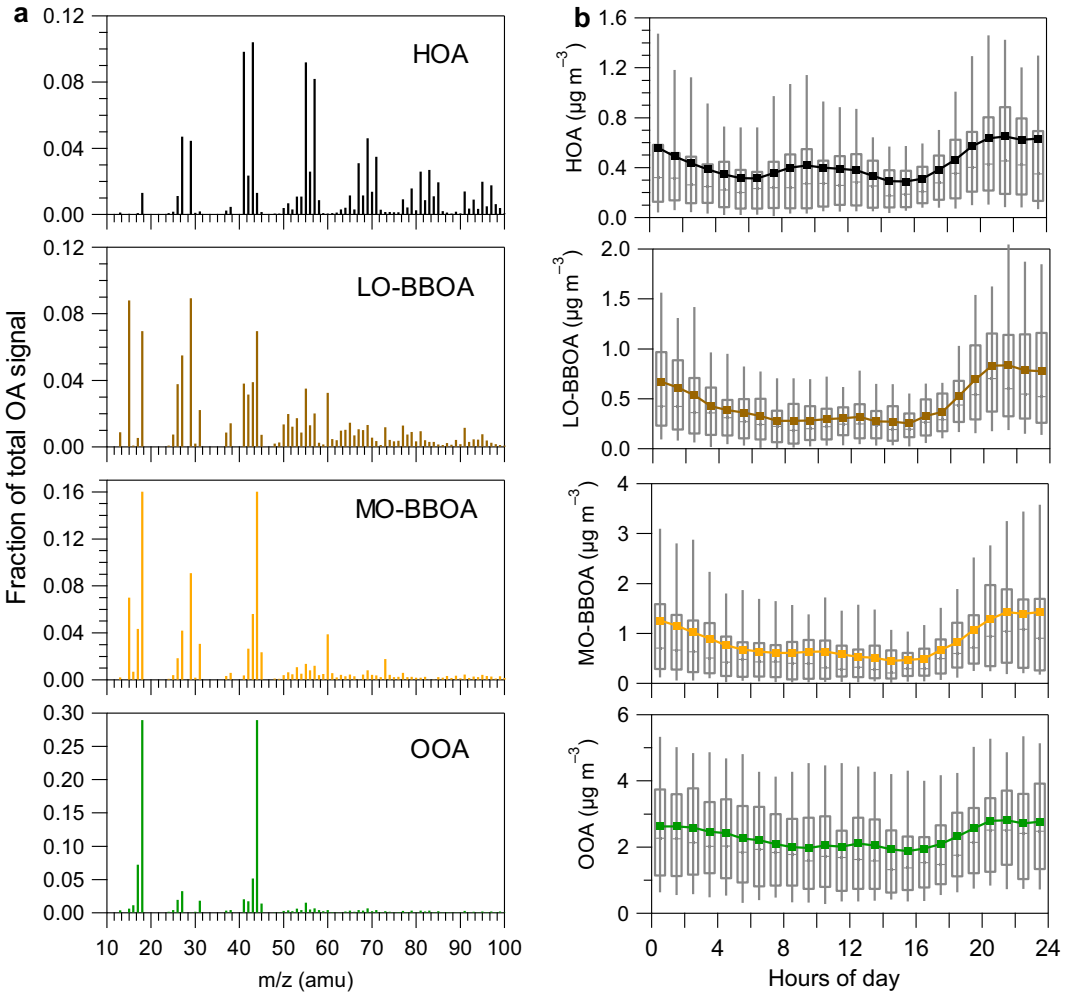

Fig. 6. Mass spectra and diel variations of the four OA factors, including hydrocarbon-like OA (OA), low oxidized biomass burning OA (LO-BBOA), more oxidized BBOA (MO-BBOA), and oxygenated OA (OOA), obtained from the PMF ACSM OA dataset observed at SIRTA. The upper and lower boundaries of boxes indicate the 75th and 25th percentiles, respectively; the lines within the box correspond to median values; the whiskers above and below boxes refer to 95th and 10th percentiles, respectively; and solid lines represent mean values.

shows a very good correlation with BBOA used in Zhang et al. (2019) (Fig. S4e). These results further support that our two-factor BBOA solution could be associated with residential wood burning emissions sector (Denier van der Gon et al., 2015; Zhang et al., 2019).

The mass spectrum of OOA is characterized by a dominate peak at m/z 44 (Fig. 6a), which has been observed worldwide in urban environments (Crippa et al., 2014; Daellenbach et al., 2017; Jimenez et al., 2009; Zhang et al., 2011). As shown in Fig. 6b, OOA exhibits high mass concentrations during nighttime with a similar diurnal trend as biomass burning aerosols. As shown in Fig. S4f, OOA also has an excellent correlation ($r^2 = 0.97$, slope $= 1.0$) with the total OOA that is from (Zhang et al., 2019), supporting that our new PMF factor solution can fully explain the OOA factor fraction. As presented in Zhang et al. (2019), we have demonstrated that the wintertime OOA factor could be substantially influenced by local-and/or small regional-scale residential wood burning emissions (Zhang et al., 2019). In fact, such a OOA factor, relevant to biomass burning source, has been also widely observed in some western Europe regions during wintertime (Bozzetti et al., 2017; Daellenbach et al., 2017).

Fig. 7 presents the PSCF value distributions for different PMF OA factors observed at SIRTA. As Fig. 7a shows, the high PSCF values for LO-BBOA are mainly distributed in the area near the sampling site, indicating that local-scale wood burning emissions could significantly contribute to the high concentration of freshly-generated BBOA at SIRTA. In addition, a small high-PSCF region was observed located to the southeast of the sampling site, suggesting potential contribution of short-distance transport to LO-BBOA observed at SIRTA. Compared to LO-BBOA, MO-BBOA presents a larger high-PSCF region, including local and the area from the south to southeast of the Paris region (see Fig. 7b). This highlights that the important sources of the more oxidized BBOA could be associated with local emissions and regional transport of residential wood burning. Moreover, these results could help to partly explain the different oxidation state for these two BBOA factors. For example, LO-BBOA could be considered as a freshly-generated factor mainly from local emissions, while MO-BBOA could represent for a more processed factor that was formed during regional transport and/or by rapid oxidation transformation once its precursors are emitted into the atmosphere (Nalin et al., 2016). Nevertheless, it's worthful for further investigating more detailed formation mechanism of these two BBOA factors in further study. As shown in Fig. 7c, HOA presents a highly similar PSCF pattern as the two BBOA factors, which is characterized by high values associated with both the local scale and the region located to the south and southeast of the sampling site. This is mainly due to that the HOA factor here is a mixed OA factor emitted from fossil fuel and biomass combustion, which has been demonstrated by some previous studies performed at SIRTA (Petit et al., 2014; Srivastava et al., 2018; Zhang et al., 2019). Interestingly, as shown in Fig. 7d, OOA also presents a very similar PSCF pattern as the two BBOA factors. This could support that the formation of high concentration of this SOA factor could be linked to wood burning source sector from local scale and regional transport. This result is also consistent with our previous findings that high concentration of wintertime OOA was mainly associated with wood burning source (Zhang et al., 2019).

3.4. Sources and optical properties of BrC at SIRTA

BrC sources could be further examined at SIRTA using outputs of the specific PMF analysis performed on the OA mass spectra obtained from ACSM measurements in winter 2014–2015 and applying MLR to $b_{BrC,370}$ data (see Section 2.5). BrC absorption coefficients estimated from this

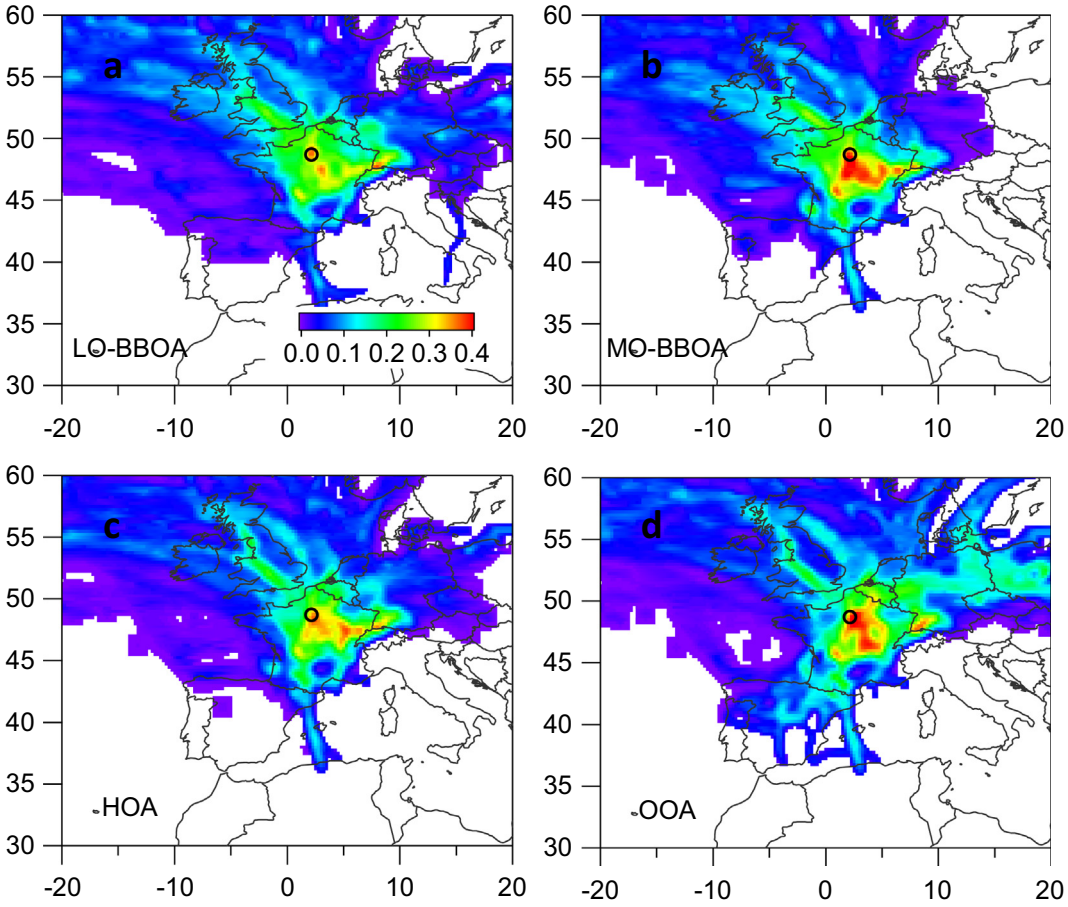

Fig. 7. Potential geographic sources of PMF OA factors, including (a) LO-BBOA, (b) MO-BBOA, (c) HOA and (d) OOA, observed at SIRTA. The PSCF values are indicated by color scales, where a color scale bar is only shown in the top-left panel.

MLR analysis are quite consistent with those measured at different wavelengths (Fig. S2), indicating that the four OA factors can reasonably explain total BrC absorption coefficients. As shown in Fig. 8a, the main BrC contributors were found to be the two biomass burning OA factors (with more than 40% and 30% of total BrC absorption for LO-BBOA and MO-BBOA, respectively), followed by OOA (18%), and HOA (8%) on averages, reinforcing our conclusion that biomass burning was the predominant BrC source at SIRTA.

Fig. 8b presents wavelength-dependent MAE of the PMF OA factors in the range 370–660 nm, and subsequent AAE values, as retrieved from MLR analysis at the different wavelengths (see also Table S3). AAE values obtained for BrC attributed to the two BBOA factors (i.e., about 8.8 and 6.6 respectively for MO-BBOA and LO-BBOA) are much higher than the ones obtained for OOA (3.45) and then HOA (2.75). This indicates a more significant wavelength dependence of biomass burning brown carbon aerosols than any of OOA and HOA. As a matter of fact, OA emitted from primary biomass burning contains the largest part of brown carbon chromophores which strongly absorb light at near-UV wavelengths (Huang et al., 2018; Kumar et al., 2018; Lu et al., 2015; Wang et al., 2019). Moreover, the stronger wavelength dependence obtained for MO-BBOA (compared to LO-BBOA, which can be considered as fresher emissions) is consistent with the features of primary vs. secondary biomass burning OA (or oxidized primary OA) reported by Saleh et al. (2014).

Regarding absorptivity, the MAE at 370 nm of LO-BBOA was of 4.85 ± 0.18 m^2 g^{-1}, which is in agreement with the value of freshly-generated BBOA from wood burning laboratory experiments (Kirchstetter et al., 2004; Kumar et al., 2018). Compared to LO-BBOA, a lower MAE (2.02 ± 0.12 m^2 g^{-1}) was estimated for MO-BBOA (a more oxidized biomass burning factor), which is comparable to aged brown carbon particles generated from a wood burning chamber experiment (Kumar et al., 2018). These results evidence that the less oxidized BBOA has stronger effective absorptivity than the more oxidized BBOA, as previously observed by other studies in ambient air (de Sá et al., 2019). The calculated HOA MAE at 370 nm is of 1.06 ± 0.23 m^2 g^{-1}, which is higher than the value observed for HOA in tunnel environment in Zurich (below 0.4 m^2 g^{-1}) (Moschos et al., 2018). This can be partly explained by the fact the HOA factor at SIRTA is not made of traffic-emitted organic aerosols only during cold months and can be mixed with biomass burning organic aerosols (Petit et al., 2014; Srivastava et al., 2018; Zhang et al., 2019).

Finally, to evaluate the potential climate implications of residential wood burning BrC absorption observed in the conditions of the present study, we performed simplified BC and BBOA radiative effect calculations. More description and equations used for these calculations are given in Text S2. Briefly, the real refractive index and mean diameter of BrC particles were held constant at 1.55 and 160 nm, respectively. The imaginary part of refractive index of brown carbon aerosols from biomass burning emissions (k_{OA}) can be parameterized using the BC-to-OA ratio (see Text S2) (Lu et al., 2015; Saleh et al., 2014). This means that variations in the calculated radiative effect of BrC were driven by wavelength-dependent k_{OA} in this calculation. In the present work, we used of the eBC$_{wb}$-to-BBOA ratio, in good agreement with the data treatment strategy used recently by Lu et al. (2015). A minimum and maximum range (0.10–0.95) of eBC$_{wb}$-to-BBOA ratios were estimated considering BBOA to be equivalent to the two BBOA factor cases: i) the only LO-BBOA from fresh emissions and ii) the sum of both of fresh and more oxidized fractions, respectively. Such a range is in accordance with the ones commonly obtained from field and simulation chamber experiments (from ~0.01 up to ~1) (Lu et al., 2015; Saleh et al., 2014). In the present study, it was assessed to be associated with a 30–70% uncertainty range in the k_{OA} calculation and then within BrC direct radiative forcing estimates. As illustrated by Fig. 9, these calculations indicated an increase of up to approximately 40% of the direct radiative effect associated to BBOA, when these compounds are treated as light-absorbing species (using absorption property parameters estimated hereabove).

4. Conclusions

From our 9-site observations, we observed high BrC contributions to total aerosol absorption at near-ultraviolet wavelengths. Furthermore, BrC absorption coefficient at 370 nm showed an excellent correlation with levoglucosan concentrations across all sampling sites, highlighting the predominant influence of wood burning emissions onto ambient air BrC concentrations and suggesting that BrC could be used as an efficient proxy to estimate biomass burning aerosol concentrations at those sites during wintertime. The latter result might find practical applications for air quality purposes. Further studies are still needed to evaluate the robustness of such a tracer method at other locations. The distinct BrC diel patterns with peaks during late evening at all sites, supporting the importance of local residential wood burning in contributing to ambient brown carbon aerosols. Moreover, potential source analysis suggested that high BrC loadings could be substantially originated from local and/or small-reginal wood burning emissions. We also observed that the less oxidized BBOA fraction is associated with a stronger effective

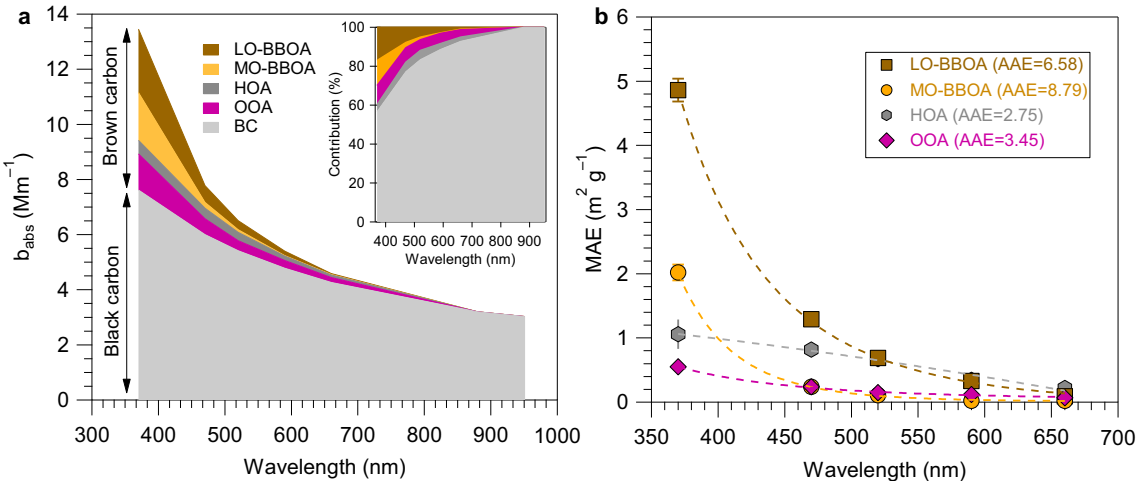

Fig. 8. (a) Wavelength dependence of average absorption coefficients (b_{abs}) and relative contributions of different absorbing aerosols to the total b_{abs} (in sub-plot) during wintertime at SIRTA. (b) Mass absorption efficiency (MAE) of the OA components obtained at SIRTA. AAE values obtained for each OA component in the 370–660 nm wavelength range are indicated within brackets.

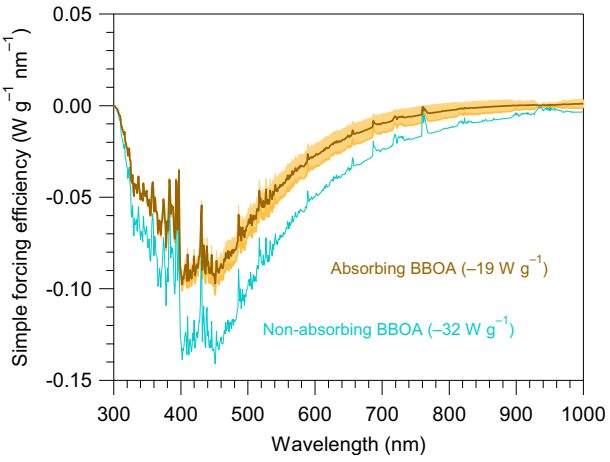

Fig. 9. Simple forcing efficiency (SFE) of BBOA (with absorbing and non-absorbing properties) at the conditions of the present study. For the absorbing BBOA properties, lower and upper bands are showing the range of the BBOA SFE corresponding to minimum and maximum estimation of refractive imaginary part index of brown carbon aerosols (see Text S2), along with the average values (solid brown line).

absorptivity than more oxidized BBOA in the Paris region. Furthermore, the wavelength-dependent mass absorption efficiencies obtained for BrC associated to both of the BBOA fractions was found to substantially influence the overall direct radiative forcing of biomass burning aerosols. A stronger regulation of residential wood burning emissions over France (and more largely over Europe, and globally) may then favorably influence not only air quality but also the climate at a regional scale during wintertime.

Data availability

Online AE33 and ACSM measurements that have been performed at the SIRTA facility are available through the ACTRIS Data Centre web portal (https://actris.nilu.no, last access: 11th March 2020). Other datasets (including 9-site brown carbon absorption and PM_{10} filters, as well as SIRTA ACSM PMF organic aerosol factors) are available at https://www.researchgate.net/publication/339831243_BrC_data_9_French_sites_2014-2015winter, doi: 10.13140/RG.2.2.21813.63200 (last access: 11th March 2020).

Funding

This research has been supported by the EU FP7 and H2020 ACTRIS projects (grant nos. 262254 and 654109), by the National Center for Scientific Research (CNRS), by the French alternatives energies and Atomic Energy Commission (CEA), and by the French ministry of Environment through its funding to the reference laboratory for air quality monitoring (LCSQA).

CRediT authorship contribution statement

Yunjiang Zhang: Conceptualization, Methodology, Software, Formal analysis, Writing - original draft, Writing - review & editing. **Alexandre Albinet:** Supervision, Writing - review & editing. **Jean-Eudes Petit:** Software, Writing - review & editing. **Véronique Jacob:** Data curation, Validation. **Florie Chevrier:** Data curation, Validation. **Gregory Gille:** Data curation, Validation. **Sabrina Pontet:** Data curation, Validation. **Eve Chrétien:** Data curation, Validation. **Marta Dominik-Sègue:** Data curation, Validation. **Gilles Levigoureux:** Data curation, Validation. **Griša Močnik:** Writing - review & editing. **Valérie Gros:** Supervision, Writing - review & editing. **Jean-Luc Jaffrezo:** Data curation, Validation, Writing - review & editing. **Olivier Favez:** Supervision, Conceptualization, Methodology, Writing - original draft, Writing - review & editing.

Declaration of competing interest

The authors declare the following financial interests/personal relationships which may be considered as potential competing interests: Griša Močnik was employed by the manufacturer of the AE33 during the measurements, but not during the data analysis or writing of the manuscript.

Acknowledgments

Y.Z. acknowledges the China Scholarship Council (CSC) for PhD scholarship.

Appendix A. Supplementary data

Supplementary data to this article can be found online at https://doi.org/10.1016/j.scitotenv.2020.140752.

References

Andreae, M.O., Gelencsér, A., 2006. Black carbon or brown carbon? The nature of light-absorbing carbonaceous aerosols. Atmos. Chem. Phys. 6, 3131–3148.
Bond, T.C., Doherty, S.J., Fahey, D.W., Forster, P.M., Berntsen, T., DeAngelo, B.J., et al., 2013. Bounding the role of black carbon in the climate system: a scientific assessment. J. Geophys. Res. Atmos. 118, 5380–5552.
Bozzetti, C., El Haddad, I., Salameh, D., Daellenbach, K.R., Fermo, P., Gonzalez, R., et al., 2017. Organic aerosol source apportionment by offline-AMS over a full year in Marseille. Atmos. Chem. Phys. Discuss. 2017, 1–46.
Canonaco, F., Crippa, M., Slowik, J.G., Baltensperger, U., Prévôt, A.S.H., 2013. SoFi, an IGOR-based interface for the efficient use of the generalized multilinear engine (ME-2) for the source apportionment: ME-2 application to aerosol mass spectrometer data. Atmos. Meas. Technol. 6, 3649–3661.
Chen, Y., Ge, X., Chen, H., Xie, X., Chen, Y., Wang, J., et al., 2018. Seasonal light absorption properties of water-soluble brown carbon in atmospheric fine particles in Nanjing, China. Atmos. Environ. 187, 230–240.
Chen, Y., Xie, X., Shi, Z., Li, Y., Gai, X., Wang, J., et al., 2020. Brown carbon in atmospheric fine particles in Yangzhou, China: light absorption properties and source apportionment. Atmos. Res. 244, 105028.
Crippa, M., DeCarlo, P.F., Slowik, J.G., Mohr, C., Heringa, M.F., Chirico, R., et al., 2013. Wintertime aerosol chemical composition and source apportionment of the organic fraction in the metropolitan area of Paris. Atmos. Chem. Phys. 13, 961–981.
Crippa, M., Canonaco, F., Lanz, V.A., Äijälä, M., Allan, J.D., Carbone, S., et al., 2014. Organic aerosol components derived from 25 AMS data sets across Europe using a consistent ME-2 based source apportionment approach. Atmos. Chem. Phys. 14, 6159–6176.
Cubison, M.J., Ortega, A.M., Hayes, P.L., Farmer, D.K., Day, D., Lechner, M.J., et al., 2011. Effects of aging on organic aerosol from open biomass burning smoke in aircraft and laboratory studies. Atmos. Chem. Phys. 11, 12049–12064.
Daellenbach, K.R., Stefenelli, G., Bozzetti, C., Vlachou, A., Fermo, P., Gonzalez, R., et al., 2017. Long-term chemical analysis and organic aerosol source apportionment at nine sites in Central Europe: source identification and uncertainty assessment. Atmos. Chem. Phys. 17, 13265–13282.
de Sá, S.S., Rizzo, L.V., Palm, B.B., Campuzano-Jost, P., Day, D.A., Yee, L.D., et al., 2019. Contributions of biomass-burning, urban, and biogenic emissions to the concentrations and light-absorbing properties of particulate matter in Central Amazonia during the dry season. Atmos. Chem. Phys. 19, 7973–8001.
Denier van der Gon, H.A.C., Bergström, R., Fountoukis, C., Johansson, C., Pandis, S.N., Simpson, D., et al., 2015. Particulate emissions from residential wood combustion in Europe – revised estimates and an evaluation. Atmos. Chem. Phys. 15, 6503–6519.
Draxler, R.R., Rolph, G.D., 2003. HYSPLIT (HYbrid single-particle Lagrangian integrated trajectory) model access via NOAA ARL READY website. NOAA Air Resources Laboratory, Silver Spring, MDhttp://www.arl.noaa.gov/ready/hysplit4.html.
Drinovec, L., Močnik, G., Zotter, P., Prévôt, A.S.H., Ruckstuhl, C., Coz, E., et al., 2015. The "dual-spot" Aethalometer: an improved measurement of aerosol black carbon with real-time loading compensation. Atmos. Meas. Tech. 8, 1965–1979.
Drinovec, L., Gregorič, A., Zotter, P., Wolf, R., Bruns, E.A., Prévôt, A.S.H., et al., 2017. The filter-loading effect by ambient aerosols in filter absorption photometers depends on the coating of the sampled particles. Atmos. Meas. Tech. 10, 1043–1059.
Favez, O., Cachier, H., Sciare, J., Sarda-Estève, R., Martinon, L., 2009. Evidence for a significant contribution of wood burning aerosols to PM2.5 during the winter season in Paris, France. Atmos. Environ. 43, 3640–3644.
Favez, O., El Haddad, I., Piot, C., Boréave, A., Abidi, E., Marchand, N., et al., 2010. Inter-comparison of source apportionment models for the estimation of wood burning aerosols during wintertime in an alpine city (Grenoble, France). Atmos. Chem. Phys. 10, 5295–5314.

Fröhlich, R., Crenn, V., Setyan, A., Belis, C.A., Canonaco, F., Favez, O., et al., 2015. ACTRIS ACSM intercomparison – part 2: Intercomparison of ME-2 organic source apportionment results from 15 individual, co-located aerosol mass spectrometers. Atmos. Meas. Tech. 8, 2555–2576.
Gilardoni, S., Massoli, P., Paglione, M., Giulianelli, L., Carbone, C., Rinaldi, M., et al., 2016. Direct observation of aqueous secondary organic aerosol from biomass-burning emissions. Proc. Natl. Acad. Sci. U. S. A. 113, 10013–10018.
Golly, B., Waked, A., Weber, S., Samake, A., Jacob, V., Conil, S., et al., 2019. Organic markers and OC source apportionment for seasonal variations of PM2.5 at 5 rural sites in France. Atmos. Environ. 198, 142–157.
Huang, R.-J., Yang, L., Cao, J., Chen, Y., Chen, Q., Li, Y., et al., 2018. Brown carbon aerosol in urban Xi'an, Northwest China: the composition and light absorption properties. Environ. Sci. Technol. 52, 6825–6833.
IPCC, 2013. Climate Change 2013: The Physical Science Basis. Contribution of Working Group I to the Fifth Assessment Report of the Intergovernmental Panel on Climate Change. Cambridge University Press, Cambridge, United Kingdom and New York, NY, USA.
Jimenez, J.L., Canagaratna, M.R., Donahue, N.M., Prevot, A.S.H., Zhang, Q., Kroll, J.H., et al., 2009. Evolution of organic aerosols in the atmosphere. Science 326, 1525–1529.
Kirchstetter, T.W., Novakov, T., Hobbs, P.V., 2004. Evidence that the spectral dependence of light absorption by aerosols is affected by organic carbon. J. Geophys. Res. Atmos. 109.
Kumar, N.K., Corbin, J.C., Bruns, E.A., Massabó, D., Slowik, J.G., Drinovec, L., et al., 2018. Production of particulate brown carbon during atmospheric aging of residential wood-burning emissions. Atmos. Chem. Phys. 18, 17843–17861.
Lambe, A.T., Cappa, C.D., Massoli, P., Onasch, T.B., Forestieri, S.D., Martin, A.T., et al., 2013. Relationship between oxidation level and optical properties of secondary organic aerosol. Environ. Sci. Technol. 47, 6349–6357.
Languille, B., Gros, V., Petit, J.-E., Honoré, C., Baudic, A., Perrussel, O., et al., 2020. Wood burning: a major source of volatile organic compounds during wintertime in the Paris region. Sci. Total Environ. 711, 135055.
Lanz, V.A., Prévôt, A.S.H., Alfarra, M.R., Weimer, S., Mohr, C., DeCarlo, P.F., et al., 2010. Characterization of aerosol chemical composition with aerosol mass spectrometry in Central Europe: an overview. Atmos. Chem. Phys. 10, 10453–10471.
Laskin, A., Laskin, J., Nizkorodov, S.A., 2015. Chemistry of atmospheric brown carbon. Chem. Rev. 115, 4335–4382.
Li, B., Gasser, T., Ciais, P., Piao, S., Tao, S., Balkanski, Y., et al., 2016. The contribution of China's emissions to global climate forcing. Nature 531, 357.
Lu, Z., Streets, D.G., Winijkul, E., Yan, F., Chen, Y., Bond, T.C., et al., 2015. Light absorption properties and radiative effects of primary organic aerosol emissions. Environ. Sci. Technol. 49, 4868–4877.
Moise, T., Flores, J.M., Rudich, Y., 2015. Optical properties of secondary organic aerosols and their changes by chemical processes. Chem. Rev. 115, 4400–4439.
Moschos, V., Kumar, N.K., Daellenbach, K.R., Baltensperger, U., Prévôt, A.S.H., El Haddad, I., 2018. Source apportionment of brown carbon absorption by coupling ultraviolet–visible spectroscopy with aerosol mass spectrometry. Environ. Sci. Technol. Lett. 5, 302–308.
Nalin, F., Golly, B., Besombes, J.-L., Pelletier, C., Aujay-Plouzeau, R., Verlhac, S., et al., 2016. Fast oxidation processes from emission to ambient air introduction of aerosol emitted by residential log wood stoves. Atmos. Environ. 143, 15–26.
Ng, N.L., Herndon, S.C., Trimborn, A., Canagaratna, M.R., Croteau, P.L., Onasch, T.B., et al., 2011. An aerosol chemical speciation monitor (ACSM) for routine monitoring of the composition and mass concentrations of ambient aerosol. Aerosol Sci. Technol. 45, 780–794.
Paatero, P., 1999. The multilinear engine—a table-driven, least squares program for solving multilinear problems, including the n-way parallel factor analysis model. J. Comput. Graph. Stat. 8, 854–888.
Paatero, P., Tapper, U., 1994. Positive matrix factorization: a non-negative factor model with optimal utilization of error estimates of data values. Environmetrics 5, 111–126.
Petit, J.E., Favez, O., Sciare, J., Canonaco, F., Croteau, P., Močnik, G., et al., 2014. Submicron aerosol source apportionment of wintertime pollution in Paris, France by double positive matrix factorization (PMF2) using an aerosol chemical speciation monitor (ACSM) and a multi-wavelength Aethalometer. Atmos. Chem. Phys. 14, 13773–13787.
Petit, J.E., Favez, O., Albinet, A., Canonaco, F., 2017. A user-friendly tool for comprehensive evaluation of the geographical origins of atmospheric pollution: wind and trajectory analyses. Environ. Model. Softw. 88, 183–187.
Petit, J.-E., Pallarès, C., Favez, O., Alleman, L.Y., Bonnaire, N., Rivière, E., 2019. Sources and geographical origins of PM10 in Metz (France) using oxalate as a marker of secondary organic aerosols by positive matrix factorization analysis. Atmosphere 10, 370.
Polissar, A.V., Hopke, P.K., Paatero, P., Kaufmann, Y.J., Hall, D.K., Bodhaine, B.A., et al., 1999. The aerosol at Barrow, Alaska: long-term trends and source locations. Atmos. Environ. 33, 2441–2458.
Qin, Y.M., Tan, H.B., Li, Y.J., Li, Z.J., Schurman, M.I., Liu, L., et al., 2018. Chemical characteristics of brown carbon in atmospheric particles at a suburban site near Guangzhou, China. Atmos. Chem. Phys. 18, 16409–16418.
Romonosky, D.E., Gomez, S.L., Lam, J., Carrico, C.M., Aiken, A.C., Chylek, P., et al., 2019. Optical properties of laboratory and ambient biomass burning aerosols: elucidating black, brown, and organic carbon components and mixing regimes. J. Geophys. Res. Atmos. 0.
Saleh, R., 2020. From measurements to models: toward accurate representation of brown carbon in climate calculations. Current Pollution Reports 6, 90–104.
Saleh, R., Robinson, E.S., Tkacik, D.S., Ahern, A.T., Liu, S., Aiken, A.C., et al., 2014. Brownness of organics in aerosols from biomass burning linked to their black carbon content. Nat. Geosci. 7, 647.
Saleh, R., Marks, M., Heo, J., Adams, P.J., Donahue, N.M., Robinson, A.L., 2015. Contribution of brown carbon and lensing to the direct radiative effect of carbonaceous aerosols from biomass and biofuel burning emissions. J. Geophys. Res. Atmos. 120, 10,285–10,296.
Sciare, J., d'Argouges, O., Sarda-Estève, R., Gaimoz, C., Dolgorouky, C., Bonnaire, N., et al., 2011. Large contribution of water-insoluble secondary organic aerosols in the region of Paris (France) during wintertime. J. Geophys. Res. Atmos. 116.
Simoneit, B.R.T., 2002. Biomass burning — a review of organic tracers for smoke from incomplete combustion. Appl. Geochem. 17, 129–162.
Srivastava, D., Favez, O., Bonnaire, N., Lucarelli, F., Haeffelin, M., Perraudin, E., et al., 2018. Speciation of organic fractions does matter for aerosol source apportionment. Part 2: intensive short-term campaign in the Paris area (France). Sci. Total Environ. 634, 267–278.
Sun, Y.L., Zhang, Q., Schwab, J.J., Demerjian, K.L., Chen, W.N., Bae, M.S., et al., 2011. Characterization of the sources and processes of organic and inorganic aerosols in New York city with a high-resolution time-of-flight aerosol mass apectrometer. Atmos. Chem. Phys. 11, 1581–1602.
Waked, A., Favez, O., Alleman, L.Y., Piot, C., Petit, J.E., Delaunay, T., et al., 2014. Source apportionment of PM₁₀ in a North-Western Europe regional urban background site (Lens, France) using positive matrix factorization and including primary biogenic emissions. Atmos. Chem. Phys. 14, 3325–3346.
Wang, Y., Hu, M., Lin, P., Tan, T., Li, M., Xu, N., et al., 2019. Enhancement in particulate organic nitrogen and light absorption of humic-like substances over Tibetan Plateau due to long-range transported biomass burning emissions. Environ. Sci. Technol. 53, 14222–14232.
Washenfelder, R.A., Attwood, A.R., Brock, C.A., Guo, H., Xu, L., Weber, R.J., et al., 2015. Biomass burning dominates brown carbon absorption in the rural southeastern United States. Geophys. Res. Lett. 42, 653–664.
Weber, S., Salameh, D., Albinet, A., Alleman, L.Y., Waked, A., Besombes, J.-L., et al., 2019. Comparison of PM10 sources profiles at 15 French sites using a harmonized constrained positive matrix factorization approach. Atmosphere 10, 310.
Xie, C., Xu, W., Wang, J., Wang, Q., Liu, D., Tang, G., et al., 2019. Vertical characterization of aerosol optical properties and brown carbon in winter in urban Beijing, China. Atmos. Chem. Phys. 19, 165–179.
Xie, X., Chen, Y., Nie, D., Liu, Y., Liu, Y., Lei, R., et al., 2020. Light-absorbing and fluorescent properties of atmospheric brown carbon: a case study in Nanjing, China. Chemosphere 251, 126350.
Zanatta, M., Gysel, M., Bukowiecki, N., Müller, T., Weingartner, E., Areskoug, H., et al., 2016. A European aerosol phenomenology-5: climatology of black carbon optical properties at 9 regional background sites across Europe. Atmos. Environ. 145, 346–364.
Zhang, Q., Jimenez, J.L., Canagaratna, M.R., Allan, J.D., Coe, H., Ulbrich, I., et al., 2007. Ubiquity and dominance of oxygenated species in organic aerosols in anthropogenically-influenced northern hemisphere midlatitudes. Geophys. Res. Lett. 34.
Zhang, Q., Jimenez, J.L., Canagaratna, M.R., Ulbrich, I.M., Ng, N.L., Worsnop, D.R., et al., 2011. Understanding atmospheric organic aerosols via factor analysis of aerosol mass spectrometry: a review. Anal. Bioanal. Chem. 401, 3045–3067.
Zhang, Y.J., Tang, L.L., Wang, Z., Yu, H.X., Sun, Y.L., Liu, D., et al., 2015. Insights into characteristics, sources, and evolution of submicron aerosols during harvest seasons in the Yangtze River delta region, China. Atmos. Chem. Phys. 15, 1331–1349.
Zhang, Y., Favez, O., Canonaco, F., Liu, D., Močnik, G., Amodeo, T., et al., 2018. Evidence of major secondary organic aerosol contribution to lensing effect black carbon absorption enhancement. npj Climate and Atmospheric Science 1, 47.
Zhang, Y., Favez, O., Petit, J.E., Canonaco, F., Truong, F., Bonnaire, N., et al., 2019. Six-year source apportionment of submicron organic aerosols from near-continuous highly time-resolved measurements at SIRTA (Paris area, France). Atmos. Chem. Phys. 19, 14755–14776.